


Amelioration of Nicotine-Induced Osteoarthritis by Platelet-Derived Biomaterials Through Modulating IGF-I/AKT/IRS-I Signaling Axis

Cell Transplantation
Volume 29: 1–11
© The Author(s) 2020
Article reuse guidelines:
sagepub.com/journals-permissions
DOI: 10.1177/0963689720947348
journals.sagepub.com/home/ccl


Wen-Cheng Lo^{1,2}, Navneet Kumar Dubey^{3,4},
Feng-Chou Tsai^{5,6}, Jui-Hua Lu^{3,4}, Bou-Yue Peng^{3,7},
Pao-Chang Chiang^{3,8}, Abhinay Kumar Singh^{3,4}, Chia-Yu Wu^{9,10},
Hsin-Chung Cheng^{3,7}, and Win-Ping Deng^{3,4,11,12} 

Abstract

Besides inhalation, a few studies have indicated that the uptake of nicotine through air or clothing may be a significant pathway of its exposure among passive smokers. Nicotine is well known to exert various physiological impacts, including stimulating sympathetic nervous system, causing vascular disturbances, and inducing cell death. Therefore, we aimed to establish whether exposure of nicotine could induce articular cartilage degeneration in a mouse model of osteoarthritis (OA). We specifically assessed dose-dependent effect of nicotine *in vitro* to mimic its accumulation. Further, during the *in vivo* studies, mice subcutaneously administered with nicotine was examined for OA-associated pathologic changes. We found that nicotine significantly suppressed chondrocytes and chondrogenic markers (Sox, Col II, and aggrecan). Nicotine-treated mice also showed altered knee joint ultrastructure with reduced Col II and proteoglycans. After corroborating nicotine-induced OA characteristics, we treated this pathologic condition through employing platelet-derived biomaterial (PDB)-based regenerative therapy. The PDB significantly suppressed OA-like pathophysiological characteristics by 4 weeks. The mechanistic insight underlying this therapy demonstrated that PDB significantly restored levels of insulin-like growth factor I (IGF-I) signaling pathway proteins, especially pIGF-I R, pAKT, and IRS-I, regulating extracellular matrix synthesis by chondrocytes. Taken together, the PDB exerts regenerative and reparative activities in nicotine-mediated initiation and progression of OA, through modulating IGF-I/AKT/IRS-I signaling axis.

Keywords

nicotine osteoarthritis, platelet-derived biomaterials, IGF-I

¹ School of Medicine, College of Medicine, Taipei Medical University, Taipei, Taiwan

² Department of Neurosurgery, Taipei Medical University Hospital, Taipei, Taiwan

³ School of Dentistry, College of Oral Medicine, Taipei Medical University, Taipei, Taiwan

⁴ Stem Cell Research Center, College of Oral Medicine, Taipei Medical University, Taipei, Taiwan

⁵ Department of Surgery, School of Medicine, College of Medicine, Taipei Medical University, Taipei, Taiwan

⁶ Division of Plastic Surgery, Department of Surgery, Shuang Ho Hospital, Taipei Medical University, New Taipei City, Taiwan

⁷ Department of Dentistry, Taipei Medical University Hospital, Taipei, Taiwan

⁸ Dental Department, Wan Fang Hospital, Taipei Medical University, Taipei, Taiwan

⁹ School of Dental Technology, College of Oral Medicine, Taipei Medical University, Taipei, Taiwan

¹⁰ Division of Oral and Maxillofacial Surgery, Department of Dentistry, Taipei Medical University Hospital, Taipei, Taiwan

¹¹ Graduate Institute of Basic Medicine, Fu Jen Catholic University, Taipei, Taiwan

¹² Department of Life Science, Tunghai University, Taichung, Taiwan

Submitted: April 16, 2020. Revised: July 8, 2020. Accepted: July 15, 2020.

Corresponding Authors:

Win-Ping Deng, Stem Cell Research Center, College of Oral Medicine, Taipei Medical University, 250, Wu-Xing Street, Taipei, Taiwan 110.

Email: wpdeng@tmu.edu.tw

Wen-Cheng Lo, School of Medicine, College of Medicine, Taipei Medical University, Taipei, Taiwan, 110.

Email: dl02092012@tmu.edu.tw



Creative Commons Non Commercial CC BY-NC: This article is distributed under the terms of the Creative Commons Attribution-NonCommercial 4.0 License (<https://creativecommons.org/licenses/by-nc/4.0/>) which permits non-commercial use, reproduction and distribution of the work without further permission provided the original work is attributed as specified on the SAGE and Open Access pages (<https://us.sagepub.com/en-us/nam/open-access-at-sage>).

Introduction

Osteoarthritis (OA) is a chronic disease, which is characterized by deteriorative changes in the osteochondral unit of knee joint, comprising of cartilage, meniscus, and subchondral bone^{1,2}. The etiology of OA is multifactorial, which includes aging, heredity, obesity, smoking, and mechanical stress, such as joint overuse or injury³. Nicotine, an addictive component of cigarette smoke, has various physiological impacts, including stimulating sympathetic nervous system, causing vascular disturbances, and inducing cell death⁴. It is widely known that the nicotine exhibits the deteriorating impacts through smoking as a major pathway. However, recent studies suggest that nicotine has also been identified as dermal permeant and could be absorbed from transdermal nicotine patches, during harvesting tobacco leaves (green tobacco sickness), vaping, or nicotine-exposed cloths, thereby may contribute its substantial accumulation over a period of time^{5,6}. A case report also evidenced an acute nicotine poisoning associated with a traditional remedy for eczema⁷, while other previous reports have documented the adverse impacts of nicotine such as reduced bone metabolic activity healing, which also indicate to influence knee joint, causing OA^{8,9}. Therefore, this study initially aimed to establish a mouse model of nicotine-induced OA as described previously¹⁰. In the animal models sometimes it seems difficult to induce the chronic accumulation of toxic substances such as nicotine to observe its dose-dependent effect, and therefore, its higher doses are preferred *in vitro*. To mimic chronic accumulation-induced toxicity by employing higher doses, even previous studies have attempted to understand its effect on functional properties of human umbilical vein endothelial cells (HUVECs)¹¹, playing key role in the progression of both periodontal disease and cardiovascular disease.

Further, the goals of current therapies of OA only offer temporary and limited benefits, such as nonsteroidal anti-inflammatory drug, corticosteroids injections, hyaluronic acid (HA)-based viscosupplementation, autologous chondrocyte implantation¹², merely relieving pain with partial recovery from pathologic symptoms, but with respect to potential safety concerns, and no reliable therapy has completely restored it. Hence, the novel methods are urgently needed to effectively address the OA treatment.

Platelet-rich plasma is isolated from whole blood and has been more specifically designated as platelet-derived biomaterial (PDB) in the recent studies^{13,14}, due to their mediated therapeutic effects through released biomaterials from platelets. PDB has been employed for regenerating cartilage, owing to its secretion of multiple growth factors, in particular, transforming growth factor- β 1 (TGF- β 1) and platelet-derived growth factor (PDGF) [2]. Previously, we have demonstrated the regenerative potential of PDB through inhibition of inflammatory cytokines and promotion of chondrogenesis¹⁵. Therefore, we for the first time aimed to determine if PDB, at optimized concentrations of human plasmatic fractions, could rescue nicotine-induced OA.

Furthermore, as the intracellular signaling pathways in chondrocytes are regulated by soluble mediators and changes in cartilaginous extracellular matrix¹⁶, a clear understanding of OA-associated specific pathway is very important to identify therapeutic targets. Previous studies have shown that insulin-like growth factor 1 (IGF-1) stimulates PI-3 kinase-Akt pathway in OA, promote not only chondrocyte survival but also proteoglycan (PG) and collagen synthesis¹⁷. However, contradictory findings also showed that PI-3 kinase-Akt pathway is also stimulated by inflammatory cytokines, such as interleukin- 1β (IL- 1β), consequently increase production of matrix metalloproteinases (MMPs) in cartilaginous matrix¹⁸. Therefore, this study aimed to identify nicotine-induced initiation and progression of OA and its therapy through PDB *in vitro* and *in vivo*. We further investigated whether this therapeutic effect of PDB is associated with modulation of IGF-1/AKT/IRS-1 signaling axis.

Materials and Methods

Chondrocyte Culture, its Maintenance, and Ethics

The human chondrocytes cultures were obtained from patients who underwent joint replacement therapy. The osteoarthritic cartilage harvested from patients was turned into pieces and digested with an enzymatic solution [8 mg/ml hyaluronidase (Sigma-Aldrich, St. Louis, MO, USA), 8 mg/ml collagenase (Sigma-Aldrich), and 2.5 mg/ml trypsin (Sigma-Aldrich)] for 6 h at 37°C. The cellular suspension was centrifuged at 1,500 rpm for 5 min and resuspended into Dulbecco's modified Eagle's medium (DMEM)/F12 (Gibco BRL, New York, NY, USA) with 10% fetal bovine serum (FBS; Gibco BRL), and 1% Penicillin-Streptomycin-Amphotericin B (PSA) (Biological Industries, Beit Haemek, Israel) in a humidified atmosphere containing 5% CO₂. Thereafter, the primary OA chondrocytes were cultured, passaged, and maintained in DMEM/F12 medium.

Based on previous reports showing various inhibitory activities of nicotine against bone density¹⁹, human renal proximal tubular epithelial cells²⁰, and myoblast differentiation²¹, we firstly established *in vitro* model of nicotine (Sigma 36733) OA, by treatment of various doses of nicotine (100, 500, and 1,000 μ M) to chondrocytes (passage 2) in the culture medium. After validating OA properties in nicotine-treated chondrocytes, we further treated them with PDB for 7 days.

PDB Preparations

The PDB was prepared and quantified as described in a previous study²². Various PDB concentrations according to enzyme-linked immunosorbent assay results of TGF- β 1 were dissolved in DMEM/F12 1% FBS medium. Chondrocytes were seeded into six-well plate at a density of 5×10^5 cells/ml and treated with PDB (TGF- β 1 = 1 ng/ml)-conditioned medium, while 1% FBS was used as experimental

Table 1. List of Genes and Their Primer Sequences Used in RT-PCR.

| Gene | Primer direction | Sequence |
|----------------|------------------|--------------------------|
| Sox9 | Forward | AGACCTTTGGGCTGCCTTAT |
| | Reverse | TAGCCTCCCTCACTCCAAGA |
| Col II | Forward | CCTTCCTGCGCCTGCTGTC |
| | Reverse | GGCCCGGATCTCCACGTC |
| Aggrecan | Forward | CCGCTACGACGCCATCTG |
| | Reverse | CCCCACTCCAAAGAAGTTTT |
| MMP-1 | Forward | AGCTAGCTCAGGATGACATTGATG |
| | Reverse | GCCGATGGGCTGGACAG |
| MMP-3 | Forward | TGGCATTCACTCCCTCTATGG |
| | Reverse | AGGACAAAAGCAGGATCACAGTT |
| MMP-9 | Forward | CCTGGAGACCTGAGAACCAATC |
| | Reverse | CCACCCGAGTGTAACCATAGC |
| β -Actin | Forward | AGAGCTACGAGCTGCCTGAC |
| | Reverse | AGCACTGTGTTGGCGTACAG |

MMP: matrix metalloproteinase; RT-PCR: reverse transcription polymerase chain reaction.

control. The optical density (OD) values were noted through Multiskan RC (Labsystems, Helsinki, Finland). Further, after 7 days of nicotine treatment, the PDB was employed to assess their effect on cellular proliferation and cell numbers were evaluated with automated cell counter Countess™ (Life Technologies, Carlsbad, CA, USA).

Proliferation Assay

For determining therapeutic effects of PDB, cell proliferation was assessed after 7-day treatment with nicotine in the presence of PDB, and cell numbers were evaluated with automated cell counter Countess™ (Life Technologies).

Real-time Polymerase Chain Reaction-based Expression of Cytokines

Total RNA was extracted from cells using High Pure RNA Isolation Kit (Roche, Mannheim, Germany) according to manufacturer's instructions. Reverse transcription (RT) was performed as previously described²³. Quantitative real-time polymerase chain reaction (PCR) was performed using an ABI 7300 real-time PCR system (Applied Biosystems, Foster, CA, USA), and gene expression was calculated by the $2^{-\Delta Ct}$ or $2^{-\Delta\Delta Ct}$ method with calibration samples included in each experiment. The primers used are shown in Table 1.

Western Blotting

Cell lysis was performed in radioimmunoprecipitation assay buffer (50 mM Tris, 150 mM NaCl, 0.5% deoxycholate (DOC), 1% NP-40, and 0.1% sodium dodecyl sulfate); thereafter, total protein was extracted, denatured for 5 min at 95°C, and separated on a 10% sodium dodecyl sulfate

polyacrylamide gel electrophoresis. Further, the proteins were transferred on to the polyvinylidene difluoride membrane (Millipore, Bedford, MA, USA) and blocked with 4% bovine serum albumin (BSA) blocking buffer. The membrane was then reacted with Sox9 (ab59252, 1:500, Abcam, Cambridge, UK), Col II (ab34712, 1:1000, Abcam), IGF-1 R (9750 S, 1:500, Cell Signaling, Danvers, MA, USA), pIGF-1 R (3024 S, 1:500, Cell Signaling), AKT (GTX121937, 1:2,500, GeneTex, Irvine, CA, USA), pAKT (GTX59559, 1:1,000, GeneTex), IRS-1 (GTX78916, 1:500, GeneTex), and β -actin (GTX109639, 1:1,000, GeneTex) polyclonal antibodies. Membranes were then incubated with anti-rabbit secondary peroxidase-conjugated antibody (111-035-003; Jackson ImmunoResearch, Newmarket, UK). Additionally, the membranes reacted with AGN (MABT83, 1:500, Millipore, Billerica, MA, USA) monoclonal antibodies were then incubated with anti-mouse secondary peroxidase-conjugated antibody (115-035-003, Jackson ImmunoResearch). The bands were visualized by using enhanced chemiluminescence detection kit (WBKLS0500, Millipore, Billerica, MA, USA) and images were analyzed using Mutigel-21 (Top Bio, Taipei, Taiwan).

In Vitro Osteoarthritic Neo-cartilage Formation and Histological Examination

The neo-cartilage formation of articular chondrocyte embedded in collagen has been described in our previous study¹⁵. Neo-cartilages were then subjected to rotatory cell culture system (RCCS-4D®, Synthecon, Houston, TX, USA) and cultured in DMEM/F12 (for control group), nicotine (1,000 μ M) (for OA neo-cartilage formation), nicotine/PDB (treatment group) containing medium in a 37°C, 5% CO₂ incubator, and medium were changed every 2 days. Neo-cartilages were processed for histological analysis after 4-week culture period. Samples were first counterstained with hematoxylin and eosin (H&E) for identifying cellular distribution. Additionally, immunohistochemical (IHC) staining of Col II (Millipore, Temecula, CA, USA) and alcian blue stain for PG were conducted to examine accumulation of cartilaginous extracellular matrix (ECM).

Nicotine-induced OA Animal Model

In 8-week-old male C57BL/6 J mice, the OA was induced through subcutaneous injection of 1.5 mg/kg nicotine ($n = 5$) as followed in previous study¹⁰, while mice with no treatment were referred as the control ($n = 3$). After 1 month of nicotine induction, 10 μ l PDB (1 ng/ml) was intra-articularly administered into knee of mice ($n = 5$) once per week for 4 weeks. After another 1 month of PDB treatment, the animals were euthanized and knee joints from all groups were then isolated for histologic and IHC studies.

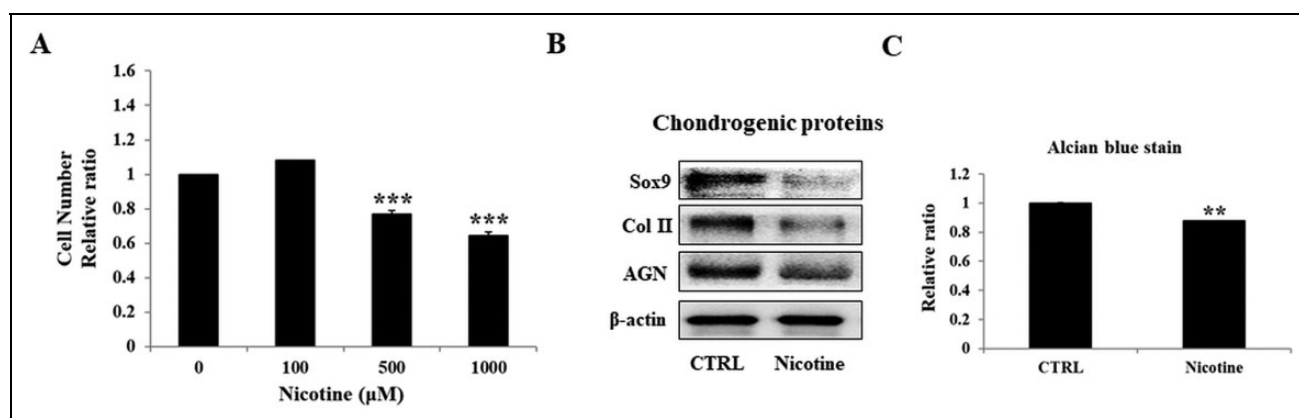


Figure 1. Effects of nicotine on cellular activity and chondrogenic markers of chondrocytes. Initially, chondrocytes were treated with nicotine doses of 100, 500, and 1,000 μM for 7 days to determine their *in vitro* proliferation ability (A). Further, due to higher damaging effect, 1,000 μM nicotine was employed in further experiments. (B) Western blotting dependent protein expressions of chondrocyte-specific markers including Sox9, Col II, and aggrecan. Further, the relative quantification of alcian blue staining (C) of control and nicotine-treated chondrocytes was done. The results are presented as mean \pm SD ($n = 3$; ** $P < 0.05$ and *** $P < 0.001$, respectively). SD: standard deviation.

Histologic and Immunohistological Staining

IHC staining was performed on fixed tissue sections using avidin–biotin peroxidase technique. Briefly, unstained sections were deparaffinized with xylene and rehydrated with decreasing concentrations of ethanol. Nonspecific binding was blocked with 4% BSA. Avidin and biotin binding sites contained in tissue samples were blocked using a commercial avidin–biotin blocking kit (Vector Laboratories, Burlingame, CA, USA). Sections were then incubated for 30 min at room temperature with following antibodies diluted in phosphate buffered saline containing BSA and incubated at 4°C for overnight. Sections were washed in ice-cold saline and incubated with a secondary biotinylated anti-mouse immunoglobulin G. The activity of endogenous peroxidase was blocked using 0.3% H_2O_2 in horseradish peroxidase (Vector Laboratories). Peroxidase activity was visualized using diaminobenzidine (Vector Laboratories). This technique uses unlabeled primary antibody, biotinylated secondary antibody, and a preformed avidin and biotinylated horseradish peroxidase macromolecular complex. The slides were further rinsed in water and lightly counterstained with hematoxylin. Besides, knee joint tissue sections were also stained with Col II and alcian blue to determine the content of cartilage and PG, respectively, in the ECM of knee joint, and OA grade was assessed using scoring system as described previously²⁴.

Statistical Analysis

Data are represented as mean \pm standard deviation for each group. The experiments were performed in triplicates, and differences between groups were estimated with Student's *t*-test and one-way analysis of variance (Sigma Plot Version

10.0 and GraphPad Prism 7). Symbols with *, **, and *** indicate $P < 0.05$, $P < 0.01$, and $P < 0.001$, respectively.

Results

Characterizing Nicotine-altered Chondrocyte Physiology

Cartilage degeneration is accompanied by various etiological factors leading to chondrocytic death. Therefore, to mimic the accumulation of nicotine during chronic exposure, higher doses of nicotine were chosen for its detrimental effect on chondrocytes. Specifically, the degenerative characteristics of cellular state were assessed after treatment with varying doses of nicotine (100, 500, and 1,000 μM) for 7 days (Fig. 1A). Compared to control, nicotine-treated chondrocytes demonstrated a significantly reduced cell numbers at 500 μM , which was further reduced in 1,000 μM concentration. Therefore, to observe higher damaging effects, the optimized dose of 1,000 μM was used in further experiments. The degenerative effect at dose of 1,000 μM was validated by western blot analysis (Fig. 1B), which revealed significantly suppressed levels of cartilage-specific proteins. Furthermore, as loss of PGs from articular cartilage is a hallmark of the osteoarthritic process²⁵, we conducted alcian blue staining, which also showed relatively feeble staining compared to control (Fig. 1C). These above results imply that nicotine adversely altered chondrocyte physiological characteristics leading to OA.

Effect of PDB on Nicotine-accelerated OA-associated Gene/Proteins

Our results showed that nicotine strongly inhibited chondrocyte cell number; however, the inhibitory effect was

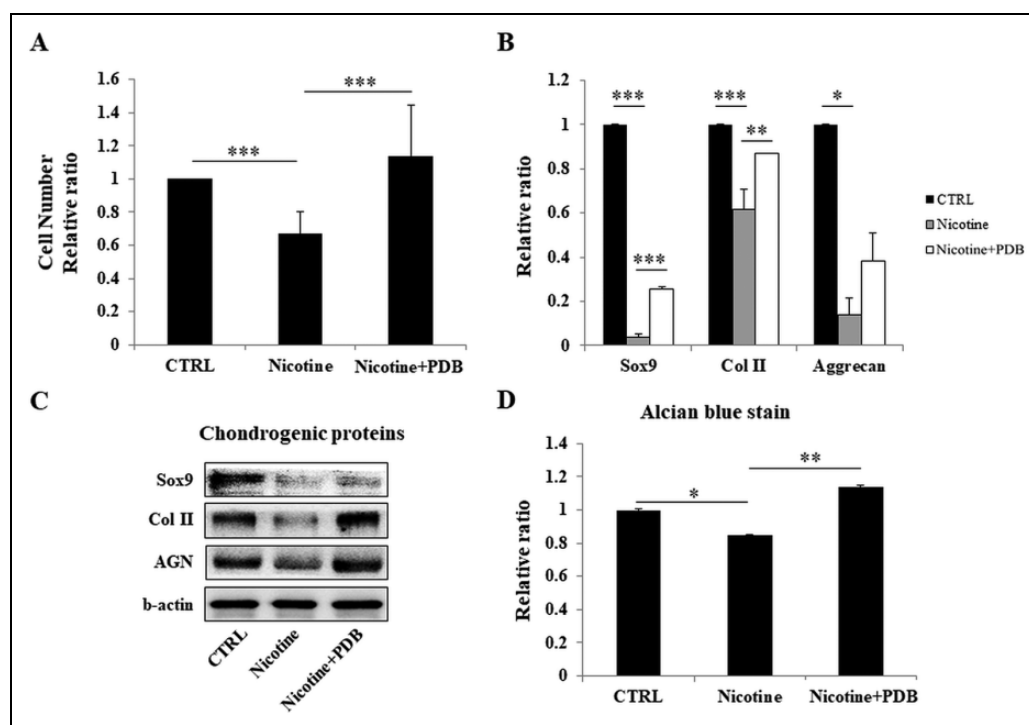


Figure 2. Influence of PDB on cellular activity and chondrogenic markers of nicotine-treated chondrocytes. After treatment with PDB for 7 days, the characteristics of chondrocytes were examined for their (A) proliferation ability, (B and C) reverse transcription and western blotting-dependent gene and protein expressions, respectively, of chondrocyte-specific markers including Sox9, Col II, and aggrecan. (D) Relative quantification of alcian blue staining of control and nicotine-treated chondrocytes. The results are presented as mean \pm SD ($n = 3$; * $P < 0.05$, ** $P < 0.01$, *** $P < 0.001$). PDB: platelet-derived biomaterial; SD: standard deviation.

reversed by PDB treatment (Fig. 2A). RT-PCR assay revealed an increased expression levels of cartilage-specific genes, including Sox9, Col II, and aggrecan (AGN) (Fig. 2B). Western blot analysis of Sox9, Col II, and AGN proteins (Fig. 2C) also followed the similar trend as of cell number and RT-PCR. These results were further supported by enhanced alcian blue staining and its quantified results in PDB-treated group (Fig. 2D).

Therapeutic Potential of PDB on Nicotine-treated Three-dimensional Neo-cartilage OA Model

In order to assess the therapeutic effect of PDB on osteoarthritic chondrocytes, a three-dimensional (3D) neo-cartilage OA model was established. H&E staining showed that compared to control group (Fig. 3A-a), the neo-cartilage treated with nicotine revealed an altered chondrocytic morphology (Fig. 3A-b) along with increased cell death, indicating osteoarthritic characteristics. However, PDB treatment not only suppressed the cell death in OA-like 3D neo-cartilage but also restored normal morphology of chondrocytes (Fig. 3A-c). Further, nicotine-treated neo-cartilage group showed a highly reduced cartilaginous ECM and glycosaminoglycans (GAGs), as demonstrated by IHC Col II (Fig. 3A-e) and alcian blue staining (Fig. 3A-h), when compared to their respective controls (Fig. 3A-d, g). However, the intense positive signals

of Col II and alcian blue implied an enhanced ECM and GAGs synthesis in PDB-treated group (Fig. 3A-f, i, respectively). These results were also confirmed through quantification of their positive signals (Fig. 4B, C, respectively).

Intra-articular Administration of PDB in Nicotine-induced OA Mouse Model

Eventually, the therapeutic potential of PDB was investigated in the *in vivo* model of nicotine-induced OA mice, as described in Fig. 4A. After 4 weeks of OA induction, the PDB was intra-articularly administered into nicotine-induced OA knee joint for further 4 weeks. H&E staining demonstrated that compared to control (Fig. 4B-a), highly reduced number of chondrocytes and lacunae appeared in wavy and disrupted collagen network in nicotine-treated knee joint (Fig. 4B-b), which were recovered through PDB treatment (Fig. 4B-c). The IHC staining for Col II in control group showed intense positive brown signals (Fig. 4B-d), whereas nicotine-treated group revealed a feeble staining (Fig. 4B-e), which was later reappeared in PDB-treated group (Fig. 4B-f). Similarly, much reduced blue staining in nicotine-treated group indicated huge loss of GAGs (Fig. 4B-h), when compared to control (Fig. 4B-g). However, an intensive blue staining signal was present in cartilaginous structure of PDB-treated group (Fig. 4B-i). Furthermore,

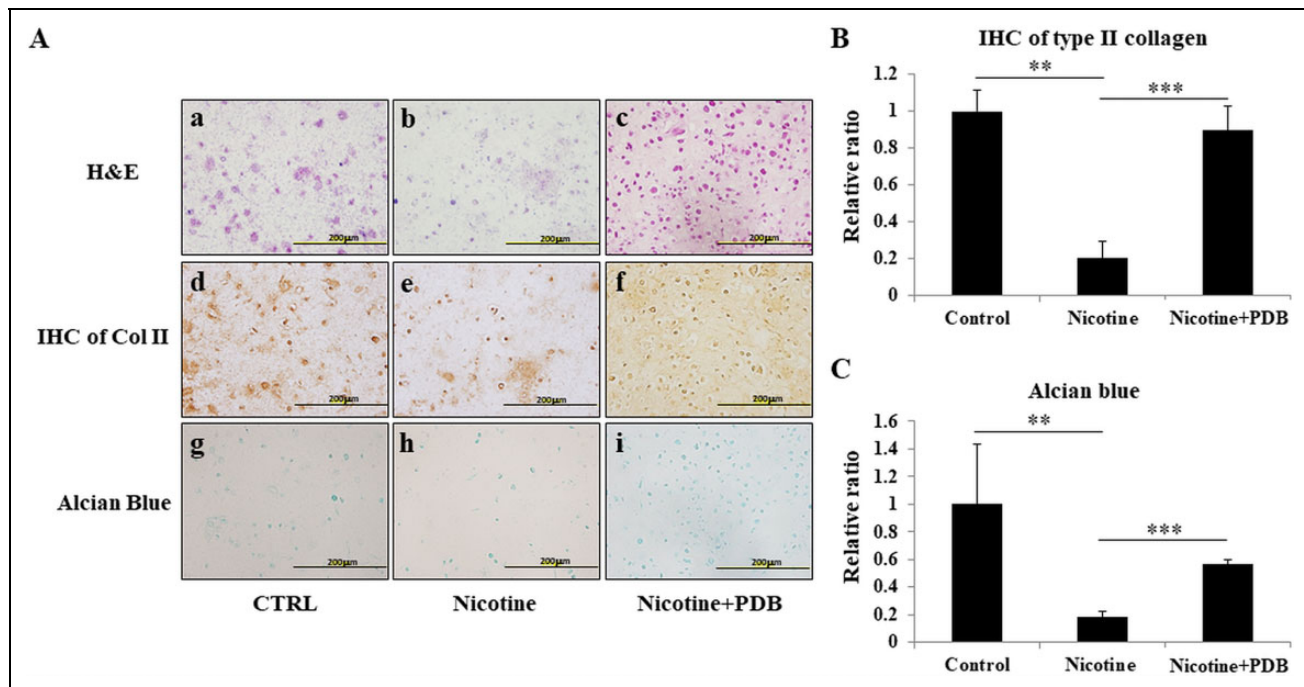


Figure 3. Determination of chondro-regenerative effects of PDB on nicotine-treated 3D neo-cartilage OA model. (A) H&E staining (a–c, upper panel), immunocytochemical staining of Col II (ICC Col II) (d–f, middle panel), and alcian blue staining (g–i, lower panel) were conducted to determine the morphologic impairments, collagen, and proteoglycan content, respectively, in synthetic cartilaginous matrices of control, nicotine-treated, and PDB-treated nicotine-OA group. All the images were obtained at $\times 20$ magnification (scale bar: 200 μm). Further, based on these stainings, the relative quantifications of (B) Col II and (C) proteoglycan were done. The results are presented as mean \pm SD ($n = 3$; $**P < 0.01$ and $***P < 0.001$, respectively). H&E: hematoxylin & eosin; OA: osteoarthritis; PDB: platelet-derived biomaterial; SD: standard deviation.

compared to control, the severity of OA after scoring was much higher in nicotine-treated group, which was significantly suppressed through PDB treatment (Fig. 4C).

Efficacy of PDB on IGF-1 R Signaling Pathway in Nicotine-induced OA Knee Joint

The IGF-1/IRS pathway has been documented to modulate PI3K/AKT phosphorylation and regulate synthesis of ECM proteins during the early development of chondrocytes¹⁷. Further, IGF-1 also functions systemically as well as locally to exhibit endocrine, paracrine, and autocrine response. Our results demonstrated that exposure of nicotine for 4 weeks suppressed protein levels of IGF-1 signaling pathway, especially pIGF-1 R (Fig. 5A), pAKT (Fig. 5B), and IRS-1 (Fig. 5C) in knee joint compared to control. However, the administration of PDB significantly restored levels of these proteins, indicating its positive effect on IGF-1 signaling pathway leading to enhanced synthesis of ECM.

PDB Intervention and Levels of Inflammatory Biomarkers in Nicotine-mediated OA Knee Joint

PI3K/AKT signaling axis has been reported to play a stimulating role in production of MMPs²⁶. Therefore, to address

role of this signaling pathway in inducing synthesis of catabolic proteases IL-1 β , MMP-1, 3, and 9 in cartilaginous matrix of nicotine-induced OA knee joint, we conducted RT-PCR analysis, which revealed increased expression levels of these inflammatory molecules compared to control group (Fig. 5D). However, the reduced expression of all MMPs was exhibited in PDB-treated group, implying its anti-inflammatory activities.

Effect of PDB on Chondrocyte-specific Markers in Nicotine-induced OA Knee Joint

Our RT-PCR results demonstrated an inhibited expression of chondrocyte-lineage-specific genes, including SOX9, Col II, and AGN in nicotine-treated group when compared to control (Fig. 5E). However, a notable increase in the levels of these genes was evidenced in PDB-administered group. These results suggest that nicotine microenvironment adversely impacted cartilage health, specifically in the form of collagen and PG loss, which were lessened through intervention of PDB through inhibiting MMPs.

Discussion

This is the first report revealing PDB efficacy on nicotine-induced OA in mouse model. Our results clearly

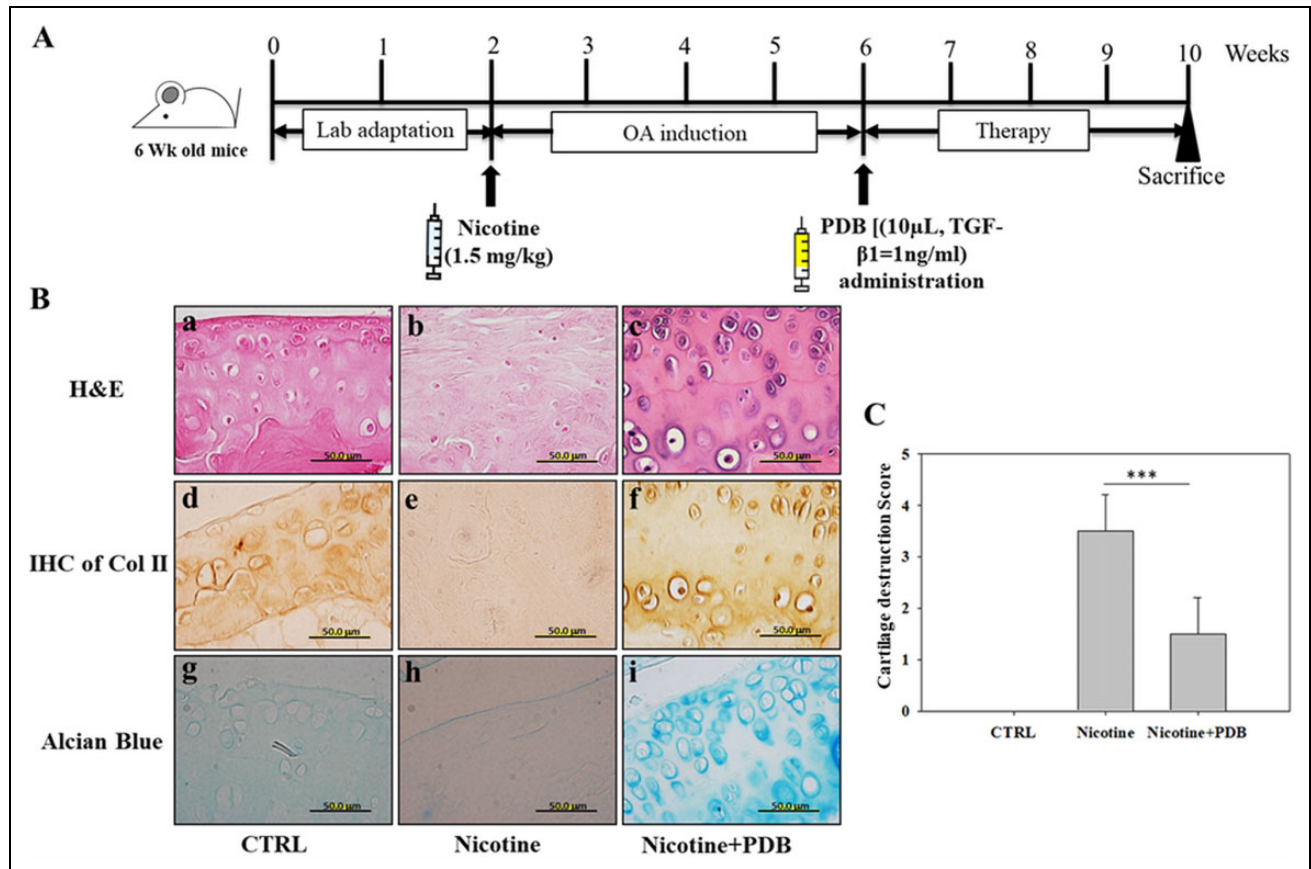


Figure 4. PDB administration and assessment of OA-associated histologic improvements. (A) Experimental protocol for PDB therapy in nicotine-induced OA mice. Following 2 weeks of lab adaptation, mice knee joint ($n = 5$) was subcutaneously injected with nicotine (1.5 mg/kg) for 4 weeks. Thereafter, PDB was intra-articularly injected in the animals ($n = 5$) once per week for 4 weeks, and the improvement in OA status was examined after further 4 weeks of treatment time. (B) Representative H&E staining (a–c, upper panel), immunohistochemical staining of Col II (IHC Col II) (d–f, middle panel), and alcian blue staining (g–i, lower panel) were conducted to determine the ultrastructural changes, collagen and proteoglycan content, respectively, in the extracellular matrix of articular cartilage of control, nicotine-treated, and PDB-treated nicotine-OA group. All the images were obtained at $\times 100$ magnification (scale bar: 50 μ m). Further, based on these histologic analyses, the severity of OA score (C) was determined. The results are presented as mean \pm SD [$n = 3$ (control); $n = 5$ (nicotine and nicotine + PDB)]; *** $P < 0.001$. H&E: hematoxylin & eosin; OA: osteoarthritis; PDB: platelet-derived biomaterial; SD: standard deviation.

demonstrated reduced chondrocyte numbers with increasing doses of nicotine, which was employed to mimic the accumulation of nicotine during chronic exposure. The RT-PCR and western blot analysis showed a suppressed expression of chondrogenic genes and proteins, respectively, including SOX9, Col II, and AGN. Additionally, the alcian blue staining showed decreased PG content, which implied nicotine-suppressed chondrogenesis. These deteriorating outcomes might also be ascribed to different isomers of nicotine. This is in line with an important study that documented that (-)-nicotine isomeric form is more active and twice toxic than (+)-nicotine²⁷. Our results are supported by study of Yang et al. showing inhibited proliferation and suppressed expression of mRNA expression of Sox9, type II collagen, and AGN in nicotine-treated group compared to control²⁸. These pathophysiological impacts strongly portend the risk of nicotine to compromise knee joint integrity and cause OA.

Further, after confirming nicotine-induced OA, we administered PDB, which is a cocktail of growth factors released from concentrated platelets, and entails various clinical applications owing to their stronger anti-inflammatory and regenerative activity²⁹. We showed that PDB-treated nicotine-induced OA group had an increased expression of chondrogenic proteins and PG content, indicating therapeutic behavior of PDB against inhibitory effect of nicotine. Interestingly, it has been documented that the nicotine as a cholinergic alkaloids act on central and peripheral nicotinic and muscarinic receptors causing central nervous system, sympathetic autonomic, parasympathetic autonomic, and neuromuscular effects in varying combinations, relying on dose of ingested substance⁷. Nicotine initially functions as an agonist at nicotinic receptor causing effects consistent with sympathetic stimulation, but then blocks the receptor producing late parasympathetic effects and neuromuscular

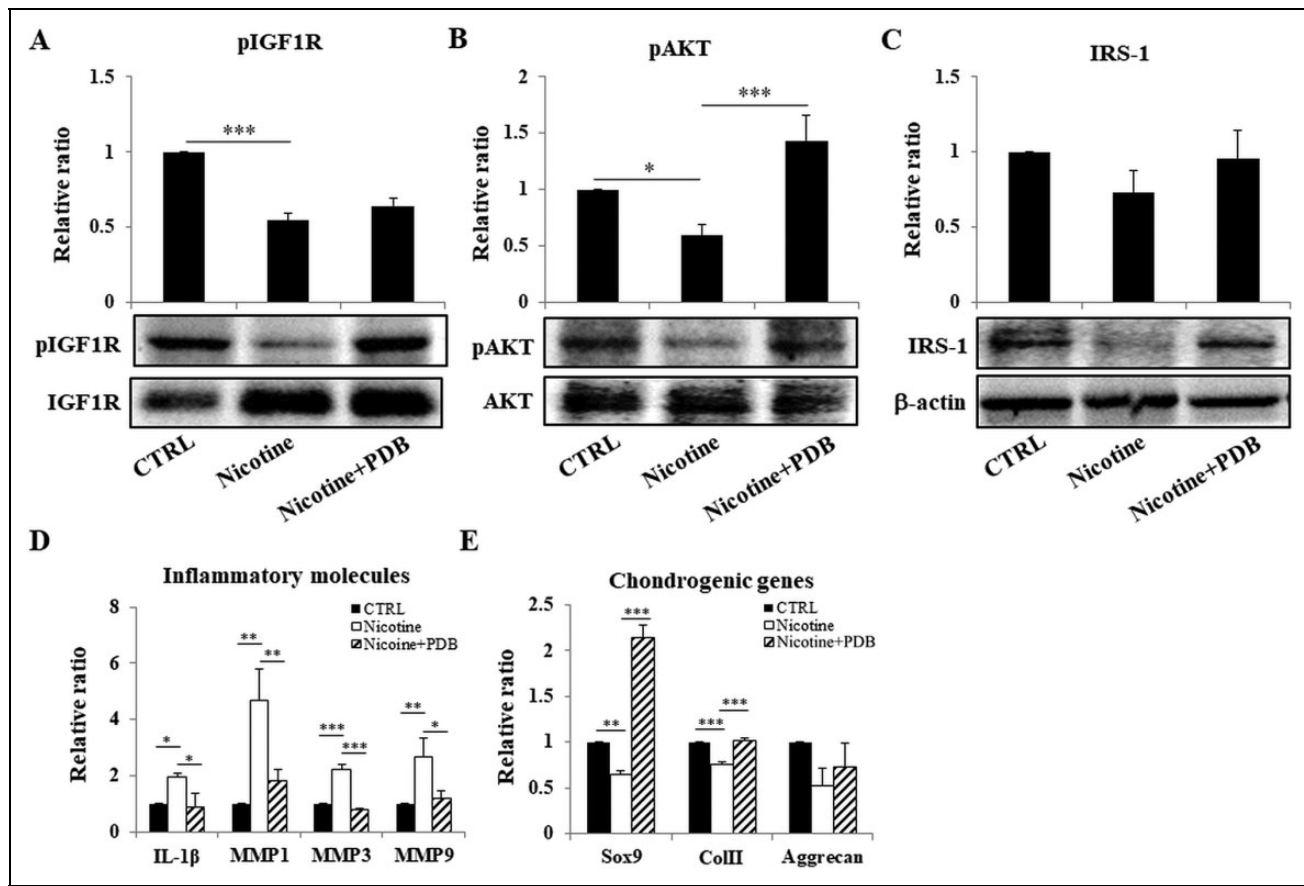


Figure 5. Efficacy of PDB on IGF-I signaling, inflammatory status, and chondrogenic proteins in knee joint. Assessment of expression levels of (A) pIGF-I, (B) pAKT, and (C) IRS-I in control, nicotine-treated, and PDB-treated nicotine-OA group. Further, in these groups, the gene expression of inflammatory mediators including IL-1 β , MMP-1, MMP-3, and MMP-9 (D) and chondrogenic genes (E) was investigated. The results are presented as mean \pm SD ($n = 3$; * $P < 0.05$, ** $P < 0.01$, *** $P < 0.001$). IGF-I: insulin-like growth factor I; IL-1 β : interleukin-1 β ; MMP: matrix metalloproteinase; OA: osteoarthritis; PDB: platelet-derived biomaterial; SD: standard deviation.

blockade. This is an indicative of nicotine-mediated actions in two phases, with the first being stimulatory, while second the inhibitory. Therefore, our *in vivo* and *in vitro* studies revealing pathological influence of nicotine, in terms of initiation as well progression of knee OA, might be attributed to predominance of inhibitory response of chronic accumulation of nicotine.

Further, it has been suggested that nicotine exposure delays chondrogenesis through downregulation of IGF-1 signaling, leading to inhibited matrix synthesis by growth plate chondrocytes³⁰. In our previous studies, we have demonstrated that 3D cultures are critical for chondrocyte survival in tissue-engineered constructs, which mimic *in vivo* micro-environment maintaining chondrocytic physiology³¹. Whereas, this study revealed nicotine-induced chondrocyte apoptosis and inhibited ECM synthesis, leading to deformed morphology of neo-cartilage. After treatment with PDB, strong Col II and Alcian blue stains indicated resynthesized and reaccumulated mature chondrogenic ECM in arthritic neo-cartilage. Collectively, PDB may

overcome nicotine-induced neo-cartilage deformation through ECM reformation, leading to recovery of chondrocytes.

Beside *in vitro* studies, the establishment of various diseases/trauma-induced OA animal model plays a key role in understanding human OA pathophysiology, which helps to develop disease-modifying therapies from preclinical to clinical trials. Therefore, we established nicotine-induced OA mouse model, which was later treated with PDB. Our H&E-stained tissue sections showed the deformed joint, degraded cartilage surfaces, collagen fibrils, and PGs in nicotine-treated group, while significant recovery through PDB treatment in this group indicated its marked healing efficacies in terms of enhanced IHC collagen type II and alcian blue stainings. Further, the huge loss of chondrocytes and PG in wavy fibrils of collagen fibers of extracellular matrix, as revealed by H&E, IHC, and alcian blue staining in nicotine-induced OA group, accounts for cartilage destruction score of over 3, which was decreased to 50% after PDB intervention. These therapeutic efficacies of PDB

might also be attributed to the anti-inflammatory activities of TGF- β 1³² and lipoxins³³, regulating repair of inflamed tissues leading to matrix restoration³⁴ and regeneration³⁵. Further, the therapeutic efficacies of PDB may also be attributed to growth factors such as hepatocyte growth factor (HGF), epidermal growth factor (EGF), and fibroblast growth factor, which are present as a cocktail.³⁶ It is further well known that the viscosity of synovial fluid is ascribed to HA, which acts as a lubricant for joint movements, leading to nearly zero coefficient of friction in joint cartilage³⁷. It has been evidenced that the PDGF primarily activates HA synthase isoform 2³⁸; therefore, through regulating the endogenous HA synthesis, PDB would restore HA levels leading to elevated cartilage protection and joint lubrication³⁹. Previous studies have also underlined the synergy between HGF and VEGF, which may likely to act cooperatively in normal physiology^{40,41}, implying a role in non-inflammatory instead of inflammatory angiogenesis^{42,43}. Hence it is possible that PDB could modify the angiogenic balance through triggering the secretion of HGF⁴⁴. In similar trend, IGF-1 and PDGF could also inhibit IL-1 β -induced cartilage degradation via downregulating NF- κ B signaling⁴⁵. In addition, PDB-contained PDGF, TGF- β , IGF-1, and EGF, which are regulators of cartilage growth, may also improve chondrocyte metabolism^{46,47}.

Further, it has already been demonstrated that a key anabolic factor, IGF-1 in adult articular cartilage, stimulates phosphorylation of cell signaling protein AKT, required for PG synthesis in healthy chondrocytes⁴⁸. In our study, we found that phosphorylated level of IGF-1, AKT, and IRS was suppressed in nicotine-treated group, which was later restored through PDB intervention. Further, the PI3K/AKT signaling axis has been reported to stimulate the production of MMPs²⁶. The secretome analysis of nicotine-treated human articular chondrocytes has been demonstrated with its pathologic effects by increased synthesis of catabolic molecules such as other interleukins and MMPs (MMP-1, -2, and -3), which are critical mediators of OA pathophysiology⁴⁹. This study also suggested that nicotine at physiological levels is not only unable to diminish this catabolic effect of IL-1, but even increases the secretion. Our previous study has also documented the higher expression of various matrix-associated inflammatory markers, including IL-1 β , MMP-1, MMP-3, and MMP-9, which were found to be significantly suppressed in nicotine-treated groups by PDB therapy.

Besides various significant therapeutic outcomes, this study includes a few limitations, such as use of higher doses of nicotine during *in vitro* assessment of its toxicity to mimic chronic accumulation in human body. However, compared to our study, even high range of doses of nicotine (10 μ M–10 mM) had been tested in the previous study to determine its impact on functional properties of HUVECs¹¹, which play an important role in the progression of both periodontal disease and cardiovascular disease. Interestingly, the HUVECs were inhibited by higher dose (10 mM) and not the lower one

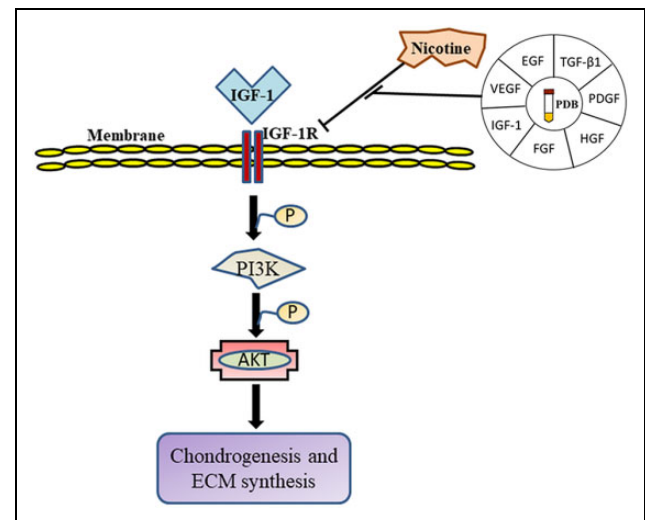


Figure 6. Schematic summary of mechanistic insight of PDB therapy in nicotine-induced OA. ECM: extracellular matrix; EGF: epidermal growth factor; FGF: fibroblast growth factor; HGF: hepatocyte growth factor; IGF-1: insulin-derived growth factor-1; OA: osteoarthritis; PDB: platelet-derived biomaterial; PDGF: platelet-derived growth factor; TGF- β 1: transforming growth factor- β 1; VEGF: vascular endothelial growth factor.

(10 μ M), implying chronic accumulation-mimicking ability of higher doses. Further, since skin is exposed to nicotine in daily life through dermal mode and uptake transdermally, we established nicotine-OA model in mice model to mimic toxicity through subcutaneous injection. Our future studies will also focus on confirming roles of other specific PDB-contained biomaterials on nicotine-induced OA. Additionally, other signaling axes will also be targeted.

Taken together, it could be inferred that PDB could efficiently inhibit nicotine-induced inflammatory profile; as a consequence, the levels of cartilage-specific genes as well proteins (SOX9, Col II, and AGN) were enhanced (Fig. 6).

Ethical Approval

All the animal care and used protocols were approved by the Institutional Animal Care and Use Committee (IACUC), Taipei Medical University, Taiwan.

Statement of Human and Animal Rights

A prior informed consent was obtained from patients and all the protocols were followed as per the Institutional Review Board (IRB No. 201305026).

Statement of Informed Consent

Verbal informed consent was obtained from the patients for their anonymized information to be published in this article.


Declaration of Conflicting Interests

The author(s) declared no potential conflicts of interest with respect to the research, authorship, and/or publication of this article.

Funding

The author(s) disclosed receipt of the following financial support for the research, authorship, and/or publication of this article: This research was funded by the following grants and agencies: Ministry of Science and Technology Taiwan (MOST 108-2221-E-038-014), Taipei Medical University (TMU 108-5601-004-111), and Stem Cell Research Center, College of Oral Medicine, Taipei Medical University, Taiwan.

ORCID iD

Win-Ping Deng  <https://orcid.org/0000-0003-2180-0472>

References

- Dubey NK, Wei H-J, Yu S-H, Williams DF, Wang JR, Deng Y-H, Tsai F-C, Wang PD, Deng W-P. Adipose-derived stem cells attenuates diabetic osteoarthritis via inhibition of glycation-mediated inflammatory cascade. *Aging Dis.* 2019;10(3):483–496.
- Dubey NK, Mishra VK, Dubey R, Syed-Abdul S, Wang JR, Wang PD, Deng WP. Combating osteoarthritis through stem cell therapies by rejuvenating cartilage: a review. *Stem Cells Int.* 2018;2018:5421019.
- Johnson VL, Hunter DJ. The epidemiology of osteoarthritis. *Best Pract Res Clin Rheumatol.* 2014;28(1):5–15.
- Zevin S, Gourlay SG, Benowitz NL. Clinical pharmacology of nicotine. *Clin Dermatol.* 1998;16(5):557–564.
- Faulkner JM. Nicotine poisoning by absorption through the skin. *J Am Med Assoc.* 1933;100(21):1664–1665.
- Benowitz NL, Lake T, Keller KH, Lee BL. Prolonged absorption with development of tolerance to toxic effects after cutaneous exposure to nicotine. *Clin Pharmacol Ther.* 1987;42(1):119–120.
- Davies P, Levy S, Pahari A, Martinez D. Acute nicotine poisoning associated with a traditional remedy for eczema. *Arch Dis Child.* 2001;85(6):500–502.
- Porter SE, Hanley EN, Jr. The musculoskeletal effects of smoking. *J Am Acad Orthop Surg.* 2001;9(1):9–17.
- Berman D, Oren JH, Bendo J, Spivak J. The effect of smoking on spinal fusion. *Int J Spine Surg.* 2017;11(4):29.
- Mangubat M, Lutfy K, Lee ML, Pulido L, Stout D, Davis R, Shin CS, Shahbazian M, Seasholtz S, Sinha-Hikim A, Sinha-Hikim I, et al. Effect of nicotine on body composition in mice. *J Endocrinol.* 2012;212(3):317–326.
- An N, Andrukhov O, Tang Y, Falkensammer F, Bantleon HP, Ouyang X, Rausch-Fan X. Effect of nicotine and porphyromonas gingivalis lipopolysaccharide on endothelial cells in vitro. *PLoS One.* 2014;9(5):e96942.
- Mora JC, Przkora R, Cruz-Almeida Y. Knee osteoarthritis: pathophysiology and current treatment modalities. *J Pain Res.* 2018;11:2189–2196.
- Arora S, Agnihotri N. Platelet derived biomaterials for therapeutic use: review of technical aspects. *Indian J Hematol Blood Transfus.* 2017;33(2):159–167.
- Yip HK, Chen KH, Dubey NK, Sun CK, Deng YH, Su CW, Lo WC, Cheng HC, Deng WP. Cerebro- and renoprotective activities through platelet-derived biomaterials against cerebrorenal syndrome in rat model. *Biomaterials.* 2019;214:119227.
- Wu CC, Chen WH, Zao B, Lai PL, Lin TC, Lo HY, Shieh YH, Wu CH, Deng WP. Regenerative potentials of platelet-rich plasma enhanced by collagen in retrieving pro-inflammatory cytokine-inhibited chondrogenesis. *Biomaterials.* 2011;32(25):5847–5854.
- Houard X, Goldring MB, Berenbaum F. Homeostatic mechanisms in articular cartilage and role of inflammation in osteoarthritis. *Curr Rheumatol Rep.* 2013;15(11):375.
- Starkman BG, Cravero JD, Delcarlo M, Loeser RF. IGF-I stimulation of proteoglycan synthesis by chondrocytes requires activation of the PI 3-kinase pathway but not ERK MAPK. *Biochem J.* 2005;389(Pt 3):723–729.
- Litherland GJ, Dixon C, Lakey RL, Robson T, Jones D, Young DA, Cawston TE, Rowan AD. Synergistic collagenase expression and cartilage collagenolysis are phosphatidylinositol 3-kinase/Akt signaling-dependent. *J Biol Chem.* 2008;283(21):14221–14229.
- Broulik PD, Rosenkrancova J, Ruzicka P, Sedlacek R, Kurcova I. The effect of chronic nicotine administration on bone mineral content and bone strength in normal and castrated male rats. *Horm Metab Res.* 2007;39(1):20–24.
- Kim CS, Choi JS, Joo SY, Bae EH, Ma SK, Lee J, Kim SW. Nicotine-induced apoptosis in human renal proximal tubular epithelial cells. *PLoS One.* 2016;11(3):e0152591.
- Lei W, Lerner C, Sundar IK, Rahman I. Myofibroblast differentiation and its functional properties are inhibited by nicotine and e-cigarette via mitochondrial OXPHOS complex III. *Sci Rep.* 2017;7:43213.
- Chen WH, Lo WC, Lee JJ, Su CH, Lin CT, Liu HY, Lin TW, Lin WC, Huang TY, Deng WP. Tissue-engineered intervertebral disc and chondrogenesis using human nucleus pulposus regulated through TGF-beta1 in platelet-rich plasma. *J Cell Physiol.* 2006;209(3):744–754.
- Wei HJ, Wu AT, Hsu CH, Lin YP, Cheng WF, Su CH, Chiu WT, Whang-Peng J, Douglas FL, Deng WP. The development of a novel cancer immunotherapeutic platform using tumor-targeting mesenchymal stem cells and a protein vaccine. *Mol Ther.* 2011;19(12):2249–2257.
- Kamekura S, Hoshi K, Shimoaka T, Chung U, Chikuda H, Yamada T, Uchida M, Ogata N, Seichi A, Nakamura K, Kawaguchi H. Osteoarthritis development in novel experimental mouse models induced by knee joint instability. *Osteoarthritis Cartilage.* 2005;13(7):632–641.
- Fosang AJ, Last K, Maciewicz RA. Aggrecan is degraded by matrix metalloproteinases in human arthritis. Evidence that matrix metalloproteinase and aggrecanase activities can be independent. *J Clin Invest.* 1996;98(10):2292–2299.
- Greene MA, Loeser RF. Function of the chondrocyte PI-3 kinase-Akt signaling pathway is stimulus dependent. *Osteoarthritis Cartilage.* 2015;23(6):949–956.
- Barlow RB, Hamilton JT. The stereospecificity of nicotine. *Br J Pharmacol Chemother.* 1965;25(1):206–212.

28. Yang X, Qi Y, Avercenc-Leger L, Vincourt JB, Hupont S, Huselstein C, Wang H, Chen L, Magdalou J. Effect of nicotine on the proliferation and chondrogenic differentiation of the human Wharton's jelly mesenchymal stem cells. *Biomed Mater Eng.* 2017;28(s1): S217–S228.
29. Chen WH, Lin CM, Huang CF, Hsu WC, Lee CH, Ou KL, Dubey NK, Deng WP. Functional recovery in osteoarthritic chondrocytes through hyaluronic acid and platelet-rich plasma-inhibited infrapatellar fat pad adipocytes. *Am J Sports Med.* 2016;44(10):2696–2705.
30. Deng Y, Cao H, Cu F, Xu D, Lei Y, Tan Y, Magdalou J, Wang H, Chen L. Nicotine-induced retardation of chondrogenesis through down-regulation of IGF-1 signaling pathway to inhibit matrix synthesis of growth plate chondrocytes in fetal rats. *Toxicol Appl Pharmacol.* 2013;269(1):25–33.
31. Chen WH, Lo WC, Hsu WC, Wei HJ, Liu HY, Lee CH, Tina Chen SY, Shieh YH, Williams DF, Deng WP. Synergistic anabolic actions of hyaluronic acid and platelet-rich plasma on cartilage regeneration in osteoarthritis therapy. *Biomaterials.* 2014;35(36):9599–9607.
32. Huynh ML, Fadok VA, Henson PM. Phosphatidylserine-dependent ingestion of apoptotic cells promotes TGF-beta1 secretion and the resolution of inflammation. *J Clin Invest.* 2002;109(1):41–50.
33. Abdul Ameer LA, Raheem ZJ, Abdulrazaq SS, Ali BG, Nasser MM, Aldeen Khairi AW. The anti-inflammatory effect of the platelet-rich plasma in the periodontal pocket. *Eur J Dent.* 2018;12(4):528–531.
34. Sundman EA, Cole BJ, Karas V, Della Valle C, Tetreault MW, Mohammed HO, Fortier LA. The anti-inflammatory and matrix restorative mechanisms of platelet-rich plasma in osteoarthritis. *Am J Sports Med.* 2014;42(1):35–41.
35. Shoeib HM, Keshk WA, Foda AM, Abo El Noeman S. A study on the regenerative effect of platelet-rich plasma on experimentally induced hepatic damage in albino rats. *Can J Physiol Pharmacol.* 2018;96(6):630–636.
36. Murata S, Maruyama T, Nowatari T, Takahashi K, Ohkohchi N. Signal transduction of platelet-induced liver regeneration and decrease of liver fibrosis. *Int J Mol Sci.* 2014;15(4): 5412–5425.
37. Seror J, Merkher Y, Kampf N, Collinson L, Day AJ, Maroudas A, Klein J. Articular cartilage proteoglycans as boundary lubricants: structure and frictional interaction of surface-attached hyaluronan and hyaluronan–aggrecan complexes. *Biomacromolecules.* 2011;12(10):3432–3443.
38. Jacobson A, Brinck J, Briskin MJ, Spicer AP, Heldin P. Expression of human hyaluronan synthases in response to external stimuli. *Biochem J.* 2000;348(Pt 1):29–35.
39. Goldring SR, Goldring MB. The role of cytokines in cartilage matrix degeneration in osteoarthritis. *Clin Orthop Relat Res.* 2004;(427 Suppl):S27–S36.
40. Xin X, Yang S, Ingle G, Zlot C, Rangell L, Kowalski J, Schwall R, Ferrara N, Gerritsen ME. Hepatocyte growth factor enhances vascular endothelial growth factor-induced angiogenesis in vitro and in vivo. *Am J Pathol.* 2001;158(3): 1111–1120.
41. Beilmann M, Birk G, Lenter MC. Human primary co-culture angiogenesis assay reveals additive stimulation and different angiogenic properties of VEGF and HGF. *Cytokine.* 2004; 26(4):178–185.
42. Min JK, Lee YM, Kim JH, Kim YM, Kim SW, Lee SY, Ghoo YS, Oh GT, Kwon YG. Hepatocyte growth factor suppresses vascular endothelial growth factor-induced expression of endothelial ICAM-1 and VCAM-1 by inhibiting the nuclear factor-kappaB pathway. *Circ Res.* 2005;96(3):300–307.
43. Gerritsen ME, Tomlinson JE, Zlot C, Ziman M, Hwang S. Using gene expression profiling to identify the molecular basis of the synergistic actions of hepatocyte growth factor and vascular endothelial growth factor in human endothelial cells. *Br J Pharmacol.* 2003;140(4):595–610.
44. Anitua E, Sanchez M, Nurden AT, Zalduendo M, de la Fuente M, Azofra J, Andia I. Reciprocal actions of platelet-secreted TGF-beta1 on the production of VEGF and HGF by human tendon cells. *Plast Reconstr Surg.* 2007;119(3):950–959.
45. Montaseri A, Busch F, Mobasheri A, Buhmann C, Aldinger C, Rad JS, Shakibaei M. IGF-1 and PDGF-bb suppress IL-1beta-induced cartilage degradation through down-regulation of NF-kappaB signaling: involvement of Src/PI-3K/AKT pathway. *PLoS One.* 2011;6(12):e28663.
46. Makower AM, Wroblewski J, Pawlowski A. Effects of IGF-I, rGH, FGF, EGF and NCS on DNA-synthesis, cell proliferation and morphology of chondrocytes isolated from rat rib growth cartilage. *Cell Biol Int Rep.* 1989;13(3):259–270.
47. Asanbaeva A, Masuda K, Thonar EJ, Klisch SM, Sah RL. Regulation of immature cartilage growth by IGF-I, TGF-beta1, BMP-7, and PDGF-AB: role of metabolic balance between fixed charge and collagen network. *Biomech Model Mechanobiol.* 2008;7(4):263–276.
48. Loeser RF, Gandhi U, Long DL, Yin W, Chubinskaya S. Aging and oxidative stress reduce the response of human articular chondrocytes to insulin-like growth factor 1 and osteogenic protein 1. *Arthritis Rheumatol.* 2014;66(8):2201–2209.
49. Lourido L, Calamia V, Fernandez-Puente P, Mateos J, Oreiro N, Blanco FJ, Ruiz-Romero C. Secretome analysis of human articular chondrocytes unravels catabolic effects of nicotine on the joint. *Proteomics Clin Appl.* 2016;10(6):671–680.